2005

Long-term testing of trenchless pipe liners

Ever Barbero

Shalini Rangarajan

Journal of Testing and Evaluation, Nov. 2005, Vol. 33, No. 6
Paper ID JTE11982
Available online at: www.astm.org

Ever Barbero[1] *and Shalini Rangarajan*[2]

Long-Term Testing of Trenchless Pipe Liners

ABSTRACT: Due to increasing costs and inconveniences in replacing deteriorated sewer pipelines by conventional excavation methods, the trenchless or "no-dig" technology is being used extensively. In this manuscript, a testing method is proposed to determine the long-term creep behavior of encased polymer and felt-reinforced polymer liners used in sewer rehabilitation. Long-term tests are conducted on liner samples encased in steel pipes, installed by the industries participating in the research project. The thicknesses of the polymer liners are selected according to the typical use of each product in the field. Three samples each of five liner materials are tested under constant external hydrostatic pressure to find their long-term structural properties. A pressure regulator, pressure transducer, and several pressure gages at different points in the water line are used to maintain constant hydraulic pressure in the gap between the steel host and the polymer liner. A method is proposed for sealing the ends of the encased liner samples for testing. The long-term creep data are collected with strain gages bonded along the inner circumference of the liner and connected to a data acquisition system (DAS). A data reduction method is proposed to separate the membrane and bending strains in order to compute the creep compliance. The temperature of the liners is monitored continuously with the use of a thermocouple. The strain data collected from the DAS are compensated for differences in temperature throughout the period of testing, initial deformation, and coefficient of thermal expansion. Several viscoelastic models are investigated in order to fit the data. The data are used to predict the long-term modulus used in the design of trenchless rehabilitation projects.

KEYWORDS: trenchless rehabilitation, sewer pipes, pipe lining

Introduction

Nowadays, rehabilitation of existing sewer lines is done using the "trenchless" or "no-dig" technology. Conventional excavation methods are no longer being used due to high costs and traffic disruptions. In trenchless lining, a polymer or reinforced polymer is applied to the inside of the existing host pipe without disturbing the soil or any aboveground facilities. The objective is to prevent ground water from seeping into the sewer. Trenchless lining can be carried out without any excavation and using existing manholes. Several technologies offer various solutions, including thermoplastic and thermoset polymers and composites, which can be reformed or cured within the host pipe or mechanically installed to fit the host pipe.

The main purpose of the liner is to prevent water and sediment leakage into the sewer pipe. Therefore a liner encased by a host sewer pipe is mainly subjected to the external head of water that builds up once the hydraulic integrity is restored [1]. The liner may also carry some soil pressure if the host pipe is severely deteriorated [2]. Regardless of the source of external pressure, the encased liner fails by creep buckling under external pressure [3].

The objective of this research is to develop a testing procedure to conduct long-term tests on full-size (305 mm diameter × 1.83 m length) encased liner samples of different liner materials and to find the long-term time-dependent properties of the liner. The main consideration is to measure the creep compliance of the liners produced under standard industry conditions. The data obtained from the long-term test are compensated for variations in ambient temperature over the entire period of testing. Initial and time-dependent deformation modes of the liner are derived from the strain data. Creep models are fit to the long-term test data for the different liner materials.

Materials can be broadly classified into elastic, viscous, or viscoelastic materials. On the application of a sudden load, which is then held constant, the elastic material would undergo an instantaneous deformation, which would then remain constant for the loading period. The viscous material will flow at a constant rate. When the load is released, the elastic material comes back to its original state. The viscous material remains as it is. In addition to elastic and purely viscous effects, viscoelastic materials also experience some recoverable viscoelastic deformation. Upon unloading, a viscoelastic material instantly recovers the elastic deformation; then it takes time to recover the recoverable viscoelastic deformation, and retains the viscous component of deformation. Creep is observed when a polymer is stressed at a constant level resulting in a strain increase over the time period. Creep compliance $D(T, t)$ is defined as

$$D(T, t) = \varepsilon(T, t)/\sigma_0 \tag{1}$$

where σ_0 is the constant applied stress and $\varepsilon(T, t)$ is the resulting strain, T is the temperature and t is the time. The relaxation modulus is defined by the equation

$$E(T, t) = \sigma(T, t)/\varepsilon_0 \tag{2}$$

where ε_0 is the constant applied strain and $\sigma(T, t)$ is the time-dependent stress. While the relaxation modulus $E(T, t)$ is not the inverse of the creep compliance $D(T, t)$ in the time domain, at time $t = 0$ we have $E_0 = 1/D_0$. Furthermore, for a viscoelastic material of the "solid" type, we have $E_\infty = 1/D_\infty$ [4].

Manuscript received June 2, 2003; accepted for publication March 23, 2005; published Nov. 2005.

[1] Chairman and Professor, Mechanical and Aerospace Engineering, West Virginia University, Morgantown, WV 26506-6106, ever.barbero@mail.wvu.edu.

[2] Graduate Research Assistant, Mechanical and Aerospace Engineering, West Virginia University, Morgantown, WV 26506-6106.

Stiffness and stability of the liner under external hydrostatic pressure is a design limit state for all types of plastic sewer linings [3]. Since long-term buckling is an important factor to be considered for the choice of wall thickness of the liner, a vital part of lining system characterization is to determine a reliable and experimentally verified procedure to find the long-term modulus of the material. Various short-term, medium-term, and long-term tests have been conducted previously on encased polymer liners to find their buckling pressures, effect of deformities on buckling pressure, effects of geometry on buckling pressure, etc. The literature review presented here focuses on structural testing performed on encased polymer liners with emphasis on the experimental method and setup chosen for testing the encased liners.

Boot and Welch [1] conducted short-term buckling tests on 450 mm (diameter) × 10 mm (thickness) liners encased in 1 m-long and 1 m-wide steel pipes. The ends of the liner were sealed using rubber seals. Air supply was used to continuously increase the pressure between the steel pipe and the liner. The deflection of the liner at different points was measured by linear variable differential transformers (LVDTs) mounted along the inner circumference of the liner. Buckling profiles were made and the buckling pressures were determined. It was seen that liners with few or no imperfections failed at a higher pressure than the liners with many imperfections. To determine the material properties of the liner, tensile and four-point bending tests were performed on the liner samples as per the BS 2782 standard. The tests were repeated after 17 months to determine the effect of aging on the liner material. It was seen that the value of modulus of elasticity increased considerably due to aging.

Straughan et al. [5] conducted tests on encased polymer liners to determine the long-term modulus. Cured-in-place pipe (CIPP) and fold and form pipe (FFP) liners installed in steel casing were tested under hydraulic pressure such that they would buckle within a 10 000 h period. The long-term modulus was calculated from the Timoshenko and Gere [6] equation for buckling of unconfined ring:

$$P_{CR} = \frac{2K\,E_\infty}{(1-\upsilon^2)} \times \frac{1}{(d/t)^3} \tag{3}$$

where P_{CR} is the critical buckling pressure, E_∞ is the long-term modulus of elasticity of the liner, υ is the Poisson's ratio, d is the mean liner diameter, t is average liner thickness, and K is an empirical enhancement factor introduced in an attempt to account for the support provided by the host pipe and surrounding soil, taken as $K = 7$ in ASTM F 1216.

Glock [7] developed a formula directly taking into account the lateral support provided by the host pipe, which does not require any empirical enhancement factor:

$$P_{CR} = \frac{1.003\,E_\infty}{(1-\upsilon^2)} \times \frac{1}{(d/t)^{2.2}} \tag{4}$$

Straughan et al. [5] accelerated the failure by increasing the pressure to whatever value was needed to buckle the liner in less than 10 000 h. In the context of accelerated testing, this means that the acceleration factor was the pressure. The behavior of polymers is nonlinear viscoelastic over broad ranges of stresses, meaning that the behavior is not linearly proportional to stress. In general, creep strain is given by

$$\varepsilon_C = \varepsilon - \varepsilon_E = a\sigma^b t^\eta \tag{5}$$

where ε_E is the elastic strain, and a, b, η are material parameters. When $b \neq 1$, stress (pressure) cannot be used as an acceleration factor. Over narrow ranges of stress, the behavior can be approximated as linear ($b = 1$). Therefore liners must be tested at stress (pressure) levels close to those encountered in the field applications.

Chunduru et al. [8] tested circular and oval HDPE liners encased in steel pipes, to estimate the long-term modulus of HDPE liners. The ends of the encased liners were sealed by bolting together two steel plates with a Plexiglas™ plate between them. The inner steel plate fit tightly with the flared ends of the liner. Air pressure, controlled with a pressure regulator and two pressure gages at the two ends of the pipe, was increased gradually in the gap between the liner and the steel pipe, until the liner buckled. Pipes of the same diameter but different thickness had different buckling pressures. Increase in ovality reduced the critical buckling pressure. Pipe liners having the same dimensions and tested under the same conditions recorded different failure pressures, suggesting that imperfections strongly affected the buckling load of cylinders (pies) under external pressure, as explained by Godoy [9,10].

Further tests conducted on HDPE liners with varying diameter-to-radius ratios (DR) have shown that thick small-diameter liners failed faster than thick large-diameter liners, and that a factor of safety of 3 to 4 needs to be applied to the short-term buckling pressure of the liner to determine the long-term (meaning 10 000 h) resistance of the flexible liner [11]. Tests on deformed and deteriorated HDPE liners showed that the ultimate buckling resistance for a tightly formed liner may be three to six times higher than that of a deformed liner. Therefore a load factor (or factor of safety) of 4 was recommended for design of HDPE liners installed in deformed or extremely deteriorated host pipes [12].

Different methods have been used to determine the deformation of the buckled liner during the tests. Image processing methods like shining a light through one end of the liner and using a video camera at the other end to tape the deflection have been used to monitor the deformation of the liner [13]. Alders et al. [14] compared different methods to measure the deformation of the liners during the buckling tests. Simple methods like shining a light through the liner or videotaping the liner were sufficient to record patterns of failure but were inadequate to measure the exact deformation of the liner. Linear variable differential transformers were used in conjunction with a DAS to measure accurately the deformation of the plastic liner throughout the length.

In this work, the deformed shape is derived from the strain data, then a viscoelastic model is fit to the long-term test data in order to determine the long-term creep properties of the liner. There are various viscoelastic models, such as the Maxwell model, the Kelvin model, the standard solid model of Maxwell and Kelvin types, and the four-parameter model. The Maxwell model consists of a spring and dashpot in series and describes well the instantaneous elastic deformation. The Kelvin model has a spring and a dashpot in parallel and exhibits creep at a decaying rate. The standard linear solid (SLS) model describes both the instantaneous elastic deformation and creep at a decaying rate. A Maxwell type SLS model consists of a spring in parallel with the Maxwell model, and a Kelvin type SLS model has a spring in series with the damper of the Kelvin model. The four-parameter model is a combination of the Maxwell and Kelvin models.

Moore and Hu [15] studied the work done on time-dependent relaxation response of HDPE pipe liner under parallel plate loading. It was found that linear viscoelastic models provided a reasonable prediction of the response of the pipe. A multi-Kelvin model was used to find the secant modulus of the material. Farshad and Flueler [16] modeled long-term creep data using the four-parameter linear viscoelastic model, which was found to fit well the creep data obtained from long-term testing of the HDPE liner pipe. The model

consists of two combinations of spring and dashpot, one in series and one in parallel.

Material Characterization

Encased liner tests are conducted at room temperature ambient (RTA). Room temperature ambient varies with time because, in a large room, the temperature control is unable to maintain the same RTA within a tight tolerance through the year. The temperature of the samples is recorded continuously during the tests using thermocouples and a DAS. In order to compensate for temperature variations, the sensitivity of material properties to temperature must be investigated for the range of temperatures encountered during long-term testing. Such investigation involves two interacting factors, temperature and physical aging, and they are addressed next.

Time-Temperature Superposition

Viscoelastic materials display large changes in properties with changing temperature, with materials being stiffer at lower temperatures. The modulus of elasticity is equal to the relaxation modulus at a fixed time. The relaxation modulus is a function of both time and temperature (Eq 2). Keeping either the time or the temperature a constant and testing for varying modulus of elasticity is a simple task. But in order to find the effect of both time and temperature on the relaxation modulus (or on its inverse, the creep compliance, Eq 1), the time-temperature superposition principle (TTSP) is used. In TTSP, tests of short durations are conducted on the material at different temperatures [17]. The curve at one temperature is chosen as a reference and all the other curves at different temperatures are shifted over time by dividing the time with a shift factor a_T. Then, a master curve of creep compliance is obtained at the reference temperature T_R (Fig. 1). Mathematically, the compliance D at a temperature T_1 and time t is equal to the compliance at temperature T_2 and time t/a_T

$$D(T_1, t) = D(T_2, t/a_T) \tag{6}$$

with the shift factor a_T given by

$$\log(a_T) = \mu_T (T - T_R) \tag{7}$$

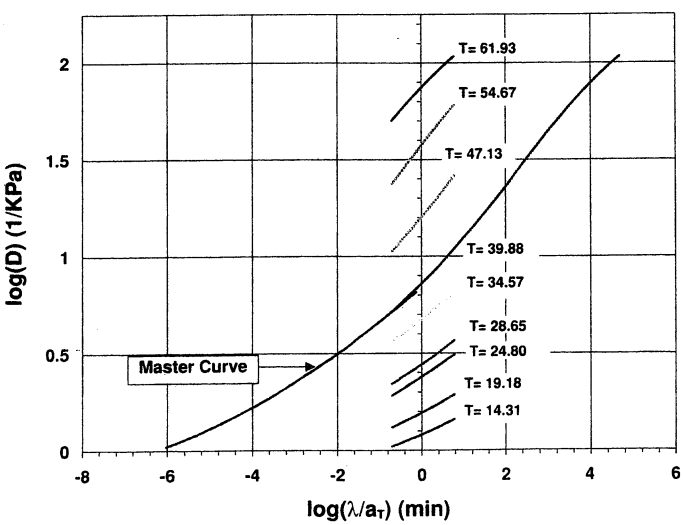

FIG. 1—*Momentary creep curves at different temperatures shifted to form TTSP master curve (Specimen A1, te = 60 min).*

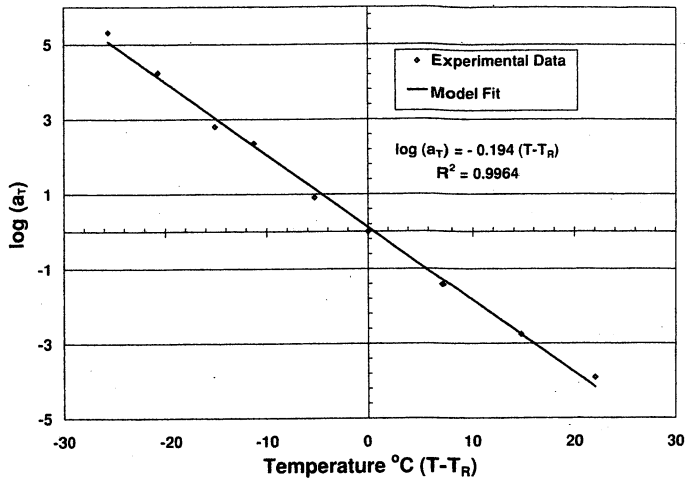

FIG. 2—*Temperature shift factor plot log (a_T) versus ($T - T_R$) (Specimen A1, te = 60 min).*

TABLE 1—*Temperature μ_T and aging μ shift factor rates [18].*

Material	μ_T	μ
A	−0.136	0.481
B	−0.113	0.720
C	−0.108	0.718
D	−0.087	0.177
E	−0.080	0.602

where the temperature shift factor rate μ_T is the slope in Fig. 2 and T_R is the reference temperature used to construct the TTSP master curve in Fig. 1. Values of the temperature shift factor rate μ_T are given in Table 1.

Physical Aging

The effect of age on the modulus of elasticity is described in this section. As the age of the material increases, the material becomes stiffer. Comprehensive aging studies on the same materials used in this investigation are reported in Refs 17 and 18. Similarly to TTSP, an aging master curve and aging shift factor plot are constructed for all materials. The slope of the aging shift factor plot is called aging shift factor rate μ, and it plays an important role in this study. The aging shift factor plot can be fitted with a straight line:

$$\log(a_e) = \mu \log(t_e - t_{eR}) \tag{8}$$

where t_{eR} is the reference age used to construct the aging master curve and a_e is the aging shift factor, which is a function of the age t_e; i.e., $a_e(t_e)$. Values of aging shift factor rate μ and temperature shift factor rate μ_T are reported in Table 1.

Long-Term Tests

Long-term compliance of polymers and polymer composites used as liners in trenchless rehabilitation is necessary for the prediction of the creep buckling of the product over its life cycle (e.g., using Eq 4). Therefore, the objective of the research was to develop a long-term full-size test method to measure the creep-compliance of liners produced under standard industry conditions. The materials in this investigation consist of five different kinds of polymer blends, reinforced and unreinforced. These materials are commercial products used for trenchless pipes and hence allow

direct comparison of the full-size test data to the actual liners in the field. The data obtained from the testing are product specific, but the methodology is applicable to the long-term behavior of a variety of polymers and polymer matrix composites.

Fabrication of Encased Liner Samples

Fabrication service was provided by the industries participating in the research. The thicknesses of the polymer liners are selected according to the typical use of each product in the field. Three specimens of each material sample are encased in 305 mm internal diameter (ID), schedule 20 (6.35 mm thickness), 1.83 m long welded steel pipes. A sample is the whole of the material from one manufacturer, produced at a given time and date. Three specimens per sample are used. The pipe liner is selected to have a length-to-diameter ratio of 6 to minimize end effects. Two 12.7 mm holes are drilled and fitted with 12.7 mm NPT female connectors welded to provide inlet and outlet. The weld line is kept halfway through the depth of the horizontally laid pipe, on the left side of the pipe while looking from the inlet end. NPT threaded bolts are placed at the inlet and outlet ports of the liner to prevent thermoset liners from sealing the inlet and the outlet during fabrication. Before lining the host pipe, a polyethylene strip is placed at each end, thus creating a space between the liner and steel host pipe (Fig. 3). The pipe is lined and cooled down as per the standard practice of the manufacturer and the polyethylene strip is removed. Round Hydrotite® is inserted in the space between the liner and steel pipe left by the polyethylene strip. Finally, epoxy grout is used to seal it completely, as shown in Fig. 3. Water is fed gently through the inlet at the bottom of the host pipe to purge the air through the top outlet. Upon contact with water, Hydrotite® expands and seals the liner against the host pipe at both ends. The samples are kept wet for one week to allow the Hydrotite® to expand completely. The testing setup is shown in Fig. 4.

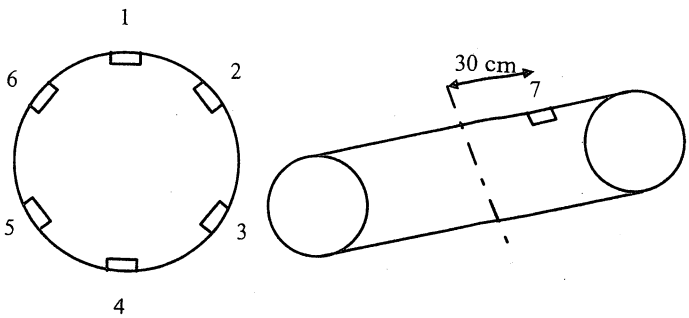

FIG. 5—*Strain gage placement in the liner sample.*

Experimental Setup

Fifteen encased liner specimens, three specimens each from each of the five manufacturers, were tested for long-term creep behavior. Strain gages are bonded onto the inside of the liner in the hoop direction of the pipe. Each liner has six gages in the center of the pipe (at 0.914 m from each end) equally spaced at an angle of 60°. In addition to the six strain gages, the first specimen of each sample has another strain gage fixed at 0.305 m from the midspan, on the inside top of the liner. The gage placement on the pipes is shown in Fig. 5.

The inlets of all the specimens are connected to a water source by CPVC tubing. The setup is such that the inlet to any sample can be individually turned on or off at any time during the testing period without disturbing the pressure on the other samples. A pressure gage with a range of 0–690 kPa is placed at the inlet of the setup to read the source water pressure. A 0–138 kPa pressure regulator controls the intensity of hydraulic pressure. A check valve is provided to prevent backflow of water. A pressure gage with a range of 0–207 kPa in the line, just after the regulator, is used to read the inlet pressure to the pipes. The outlet of each pipe is connected to a sink and can be shut on or off at any time without disturbing the

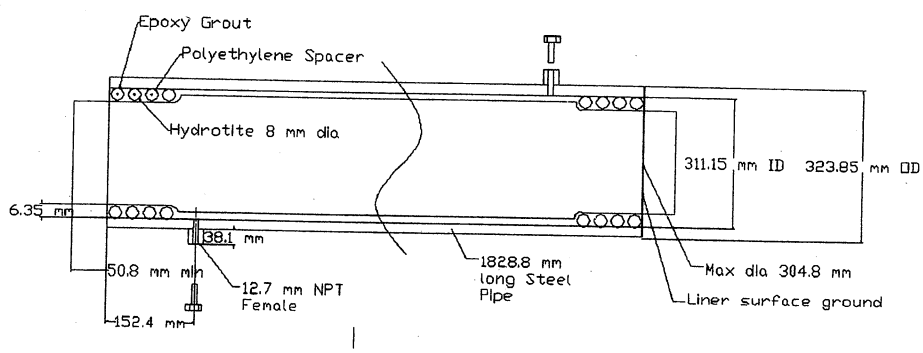

FIG. 3—*End seals with Hydrotite®, polyethylene spacer, and epoxy grout.*

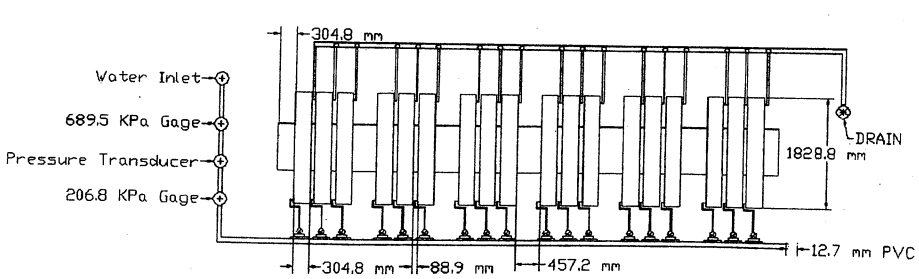

FIG. 4—*Testing installation.*

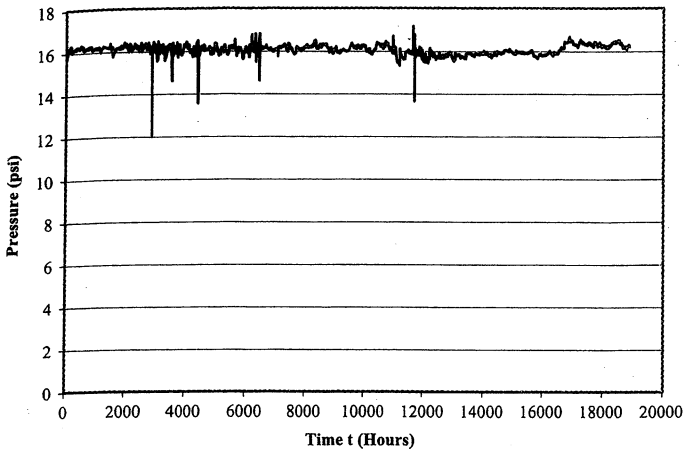

FIG. 6—*Pressure versus time for the testing period.*

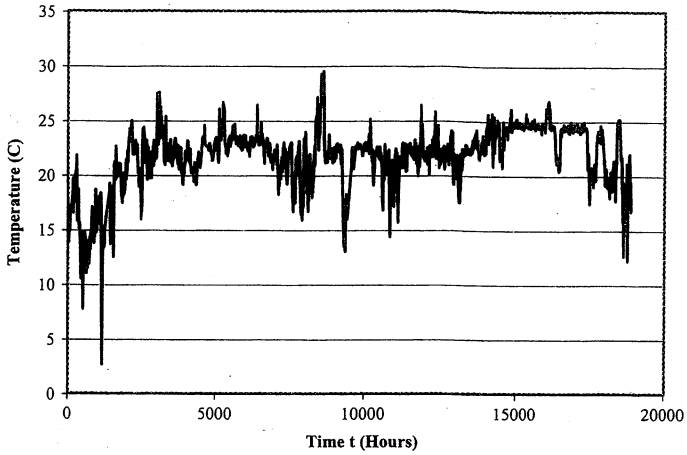

FIG. 7—*Temperature versus time for the testing period.*

other pipes. The first specimen of every sample has a pressure gage at the outlet to monitor pressure drop, if any, across the setup. A pressure transducer is provided in the water line after the pressure regulator. It is connected to a DAS and monitored and recorded continuously throughout the test. A thermocouple, attached inside the first specimen, is also connected to the DAS to continuously monitor and record the temperature of the liner. The strain gages on all the pipes are connected to the DAS so that they can be monitored and recorded continuously.

At the beginning of the test, all the strain gages are zeroed. The inlets to all the pipes are opened one at a time, keeping all outlets open. When the flow becomes steady and there are no air gaps, the outlet valve to each specimen is closed. The pipe liner samples remain at a pressure $P_o = 111$ kPa for the entire testing time. In case of a slight variation in pressure, the pressure is adjusted to $P_o = 111$ kPa by adjusting the pressure regulator. A plot of pressure variation over the testing period is shown in Fig. 6. The strain data for all gages, intensity of hydraulic pressure, and temperature are recorded into a file. The DAS software indicates when the file is full to its capacity. A new file is then started by manually stopping the recording of data momentarily and restarting the recording in a new file. A consolidation file is maintained with a collection of readings from all the data files. The consolidation file is appended periodically with data from new files.

Temperature Compensation

Since the test is long-term, there are numerous data points. A moving average is done on the data and every hundredth point is retained. Since the test is conducted over a long period of time, the testing facility is subjected to differences in ambient temperature. A plot of temperature variation over the period of testing is shown in Fig. 7. The average temperature over the first 10 000 h was 21.6°C and all results were normalized to 21.1°C (70°F). Due to temperature variations, the behavior of the material undergoes changes of creep compliance and these are reflected in the strain readings. Thus changes in ambient temperature were compensated for in the strains obtained. This was attained using a novel procedure since the classical TTSP compensation described by Eq 6 is incorrect when the data display aging effects. Therefore, the following procedure was used. The TTSP master curve (Fig. 1) and shift factor plot (Fig. 2) are constructed with a set of momentary creep curves, all of age t_e. Momentary curves contain data for a short time λ,

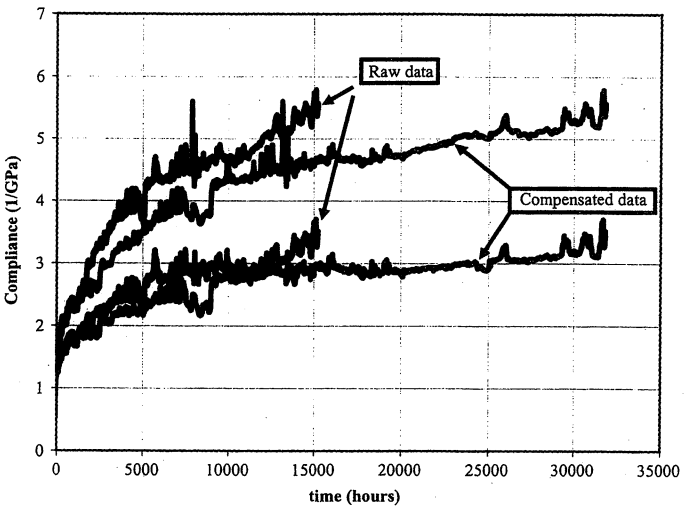

FIG. 8—*Raw strain and temperature compensated strain from one gage in each of two typical specimens.*

such that $\lambda/t_e < 1/10$. This is done so that physical aging does not contaminate the TTSP master curve [17]. Therefore, the TTSP master curve can be used only to shift data for temperature variations when the data have no physical aging [17–19]. Obviously, the long-term raw data in Fig. 8 have significant aging occurring over a test period of over 15 000 h. Each interval of time Δt in Fig. 8 is tested at time t and temperature $T(t)$, which vary with time due to the changes in the laboratory ambient conditions. The procedure to compensate the data so that it represents the behavior of the liner at a constant temperature T_R is as follows [17].

First, shift the TTSP master curve to reference $T_R = 21.1$°C and age t_{eR}. Such age t_{eR} is the time elapsed since installation of the liner in the steel host pipe at the factory (for this study) or in the field, in the case of a field installation. Next, let t_{i-1} and t_i be the beginning and end of a time interval over which the temperature T remains constant. The time t is now shifted to unaged time λ using equivalent time theory [20]:

$$\lambda = \frac{t_e}{\alpha}[(1 + t/t_e)^{\alpha} - 1] \tag{9}$$

where $\alpha = 1 - \mu$, $\mu < 1$ is the aging shift factor rate [18,19], and t_e is the age of the TTSP master curve, which has been shifted to the age of the liner t_{eR} at the onset of the encased liner test. Using Eq 9, compute the corresponding unaged times λ_{i-1} and λ_i and the

unaged interval $\Delta\lambda_i = \lambda_i - \lambda_{i-1}$ at temperature T. Now, such an interval can be adjusted to the reference temperature T_R by

$$\Delta\lambda_i = \frac{\Delta\lambda_i}{a_T} \tag{10}$$

where the temperature shift factor a_T is computed with Eq 7 and Table 1. The accumulated unaged time is computed by accumulating all the intervals as

$$\lambda'_n = \sum_{i=1}^{n} \Delta\lambda'_i \tag{11}$$

which now can be transformed to real time by

$$t'_n = \left[\frac{\lambda'_n \alpha}{t_e} + 1\right]^{\frac{1}{\alpha}} \tag{12}$$

A plot of strain versus time before and after temperature compensation for a typical gage is shown in Fig. 8.

Computation of Deflection of the Pipe Liners

The liner experiences free-ring buckling until it leans on the steel host pipe (Fig. 9). The strains grow differently for each gage depending on how this free-ring buckling mode evolves. To find the buckling modes of the liner, the deflection of the liner at the midspan has to be determined. In order to determine the deflection of the pipe liner, the strains are fit first with an equation. Since the strain distribution around the circumference is periodic with period 2π, the discrete fourier transform (DFT) is used on the available strain data. In this case, the data sampling frequency is known $(2\pi/N)$ but the equation of the waveform is not known. Hence, the strain distribution around the center inner circumference of the pipe is approximated with

$$y(\theta_r) = \frac{A_0}{2} + \sum_{n=1}^{N/2-1}\left[A_n \cos\left(\frac{2\pi rn}{N}\right) + B_n \sin\left(\frac{2\pi rn}{N}\right)\right] + \frac{A_{N/2}}{2}\cos(\pi r)$$

$$A_n = \frac{2}{N}\sum_{r=1}^{N} y(r\Delta\theta)\cos\left(\frac{2\pi rn}{N}\right) \quad n = 0, 1, \ldots, \frac{N}{2} \tag{13}$$

$$B_n = \frac{2}{N}\sum_{r=1}^{N} y(r\Delta\theta)\sin\left(\frac{2\pi rn}{N}\right) \quad n = 0, 1, \ldots, \frac{N}{2} - 1$$

where N is the number of points recorded over the sample domain $(0, 2\pi)$ at intervals of $\Delta\theta$. Equation 13 can faithfully predict features that vary with a frequency of at most $N/2$, where N is the number of sampling points. Since there are six gages around the circumference where strains are recorded, $N = 6$, and the frequency is $\Delta\theta = 2\pi/N = \pi/3$ radians. A larger value of N would be needed if features such as deflections vary rapidly in such a way that most of the feature is contained in an interval smaller than $\Delta\theta = 2\pi/N$. The value of r ranges from 0 to N. Hence, $\theta = r\Delta\theta$. Here A_n and B_n are the coefficients of the cosine and sine terms in the first part of Eq 13. Next, the term $r\Delta\theta$ in the parentheses of the cosine and sine functions is replaced by the angle θ, with $\Delta\theta = 2\pi/N$, as follows:

$$y(\theta) = \frac{A_0}{2} + A_1\cos(\theta) + B_1\sin(\theta) + A_2\cos(2\theta) + B_2\sin(2\theta) + \frac{A_3}{2}\cos(3\theta) \tag{14}$$

A plot of the actual strain data with the DFT points is shown for one gage in Fig. 10.

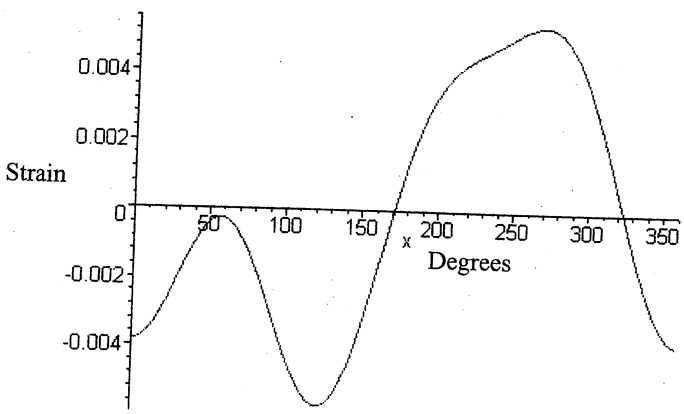

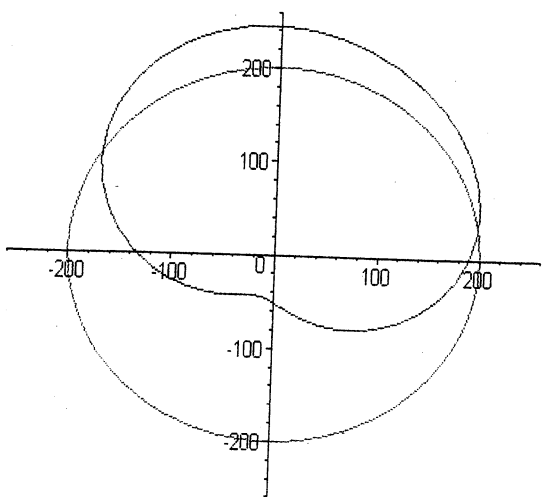

FIG. 9—*Midspan strain and deflection shape of the liner at 11 500 h for pipe A1 (deflection in mm × 100).*

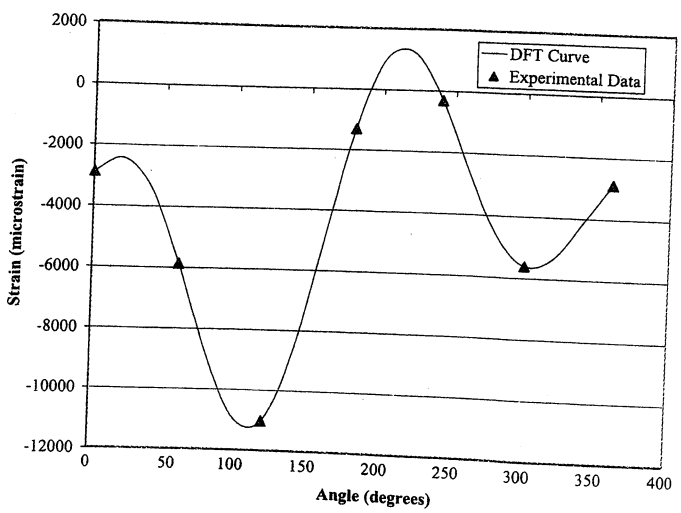

FIG. 10—*Discrete fourier transform fit of strain data from one specimen, six gages.*

The equation obtained from the above procedure is equated to $\varepsilon(\theta)$, that is, the variation of strain over the entire inner circumference. This is the total strain read by the strain gages. But this is the sum of the bending strain ε_b and membrane strain ε_m as

$$\varepsilon(\theta) = \varepsilon_b + \varepsilon_m \tag{15}$$

The membrane strain can be related to the compliance $D(t)$ by the equation

$$\varepsilon_m = -\frac{pdD(t)}{2h} \tag{16}$$

The term p is the pressure exerted on the liner pipe, d is the inner diameter of the host pipe, h is the thickness of the liner pipe, and $D(t)$ is the compliance of the liner pipe. The bending strain is proportional to the second derivative of the deflection w, and taking into account that $x = a\theta$, $x\partial^2 x = a^2\partial\theta^2$, we have

$$\varepsilon_b = -z\frac{\partial^2 w}{\partial x^2} = -\frac{z}{a^2}\frac{\partial^2 w}{\partial \theta^2} \tag{17}$$

In the above equations, $a = d/2$ is the radius of the pipe and θ is the angle at which the gages are placed. Hence, to find the deflection, Eqs 14–17 can be combined as

$$-\frac{z}{a^2}w^{II} = \frac{A_0}{2} + A_1\cos(\theta) + B_1\sin(\theta) + A_2\cos(2\theta) + B_2\sin(2\theta) + \frac{A_3}{2}\cos(3\theta) + \frac{pdD(t)}{2h} \tag{18}$$

The above equation can be rearranged to separate the periodic and nonperiodic functions

$$-\frac{z}{a^2}w^{II}(\theta) = a_0 + f(\theta) \tag{19}$$

where

$$a_0 = \frac{A_0}{2} + \frac{pdD(t)}{2h} \tag{20}$$

and

$$f(\theta) = A_1\cos(\theta) + B_1\sin(\theta) + A_2\cos(2\theta) + B_2\sin(2\theta) + \frac{A_3}{2}\cos(3\theta)$$

In the above equations, a_0 is the nonperiodic part and $f(\theta)$ is the periodic part of Eq 18. Integrating Eq 19 twice to get the deflection w, we get

$$-\frac{z}{a^2}w = a_0\theta^2 + k_1\theta + k_2 + \bar{\bar{f}}(\theta) \tag{21}$$

where k_1 and k_2 are the constants of integration and $\bar{\bar{f}}$ is the indefinite double integral of $f(\theta)$. Since the pipe must close at $\theta = 2\pi$, the following compatibility conditions must be satisfied:

$$\begin{aligned} w(0) &= w(2\pi) \\ w^{I}(0) &= w^{I}(2\pi) \end{aligned} \tag{22}$$

The periodic part $f(\theta)$ will always satisfy the above conditions, but the nonperiodic part will not satisfy the conditions. Therefore:

$$\begin{aligned} w(0) &= k_2 \\ w(2\pi) &= a_0(2\pi)^2 + k_1 2\pi + k_2 \\ w^{I}(0) &= k_1 \\ w^{I}(2\pi) &= 4\pi a_0 + k_1 \end{aligned} \tag{23}$$

The above conditions can be satisfied only if $k_1 = k_2 = a_0 = 0$. Having a_0 as zero means that, on account of Eq 20:

$$\frac{A_0}{2} = -\frac{pdD(T,t)}{2h} \tag{24}$$

Therefore, the only possible solution is that the average strain $A_0/2$ be exactly equal to the membrane strain ε_m at any time (Eq 16). This is very important because it allows us to compute the long-term compliance $D(T, t)$ as

$$D(T,t) = -\frac{A_0}{2}\frac{2h}{pd} \tag{25}$$

where $A_0/2$ is the average of the strains recorded by N gages around the circumference, halfway along the length, inside the pipe specimen. The deflection is computed from Eq 21, after substituting the values for a_0, k_1 and k_2, as

$$w(\theta) = -\frac{a^2}{h/2}\bar{\bar{f}}(\theta) \tag{26}$$

The diagram of the deflected midsection of one of the pipes is shown in Fig. 10.

Viscoelastic Model

The membrane strain is calculated by taking the average of the strains around the circumference of the liner pipe. Plots of compliance versus time are made for each specimen of each material. These are fit with a standard linear solid (SLS) viscoelastic model:

$$\begin{aligned} D(T) &= \frac{1}{E_\infty} - \left[\frac{1}{E_\infty} - \frac{1}{E_0}\right]e^{-\frac{t}{\tau}} = a + be^{-kx} \\ E_0 &= E_1 = \frac{1}{b + \frac{1}{E_\infty}} \\ \tau &= \frac{\eta}{E_2} = C = \frac{1}{k} \\ E_\infty &= \frac{1}{\left[\frac{1}{E_0} + \frac{1}{E_2}\right]} = \frac{1}{a} \end{aligned} \tag{27}$$

where E_0 is the elastic modulus, E_∞ is the long-term modulus, and η is the creep rate. The data are fit with the SLS model using the data analysis software Origin®. The R-square and chi-square values are used to decide whether the fit is a good representation of the data points. Plots of the SLS fit of the compliances of typical samples are given in Fig. 11. The values of elastic moduli E_e obtained

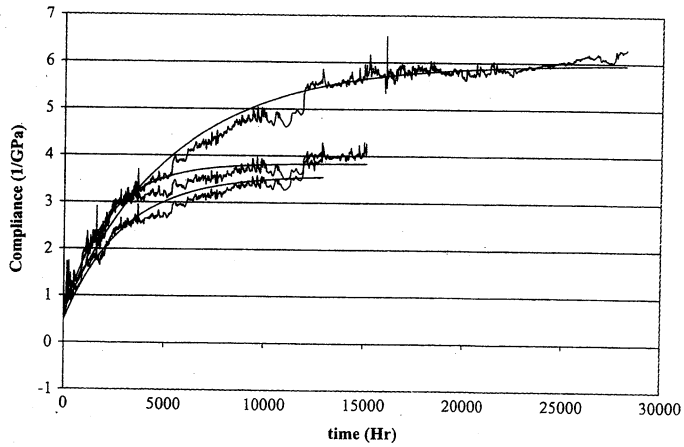

FIG. 11—*Numerical fit of the four-parameter model to the compliance data for typical samples.*

TABLE 2—*Comparison of short-term modulus from creep tests versus ASTM D 790 "as produced" samples.*

Material	ASTM D 790 E_0 (GPa)	Creep Test E_0 (GPa)
A	1.929	1.783
B	2.000	1.625
C	1.719	1.077
D	0.950	0.560
E	2.219	2.752

from fitting the long-term data are compared in Table 2 with values obtained by ASTM D 790 [21]. The values of elastic modulus of the materials obtained from long-term tests compare reasonably well with the values obtained from short-term ASTM D 790 tests, taking into account the vast differences between the two types of tests. The values of long-term moduli E_∞ can be used directly in Eq 4 for the design of trenchless rehabilitation installations.

Summary and Conclusions

The present study proposes a long-term test procedure for testing encased polymeric pipe liners used for rehabilitation of deteriorated sewer liners. The proposed test procedure can be implemented independently of the type of polymeric material used for the liner. The liner materials used for testing are commercially available materials that are used in typical field installations. Temperature compensation reduces the need for a temperature-controlled laboratory environment for such a large testing setup over such a long testing period. The deflection of the pipe liners and hence the deformation mode shapes can be computed directly from strain values using a novel procedure. Hence, the need for additional instrumentation to measure the deflection is eliminated, thereby avoiding additional costs and time. An appropriate number of gages N should be selected when features such as deflections vary rapidly over short intervals around the circumference. The viscoelastic model fits the data well, thus providing a straightforward procedure for determination of the long-term modulus, which can then be used directly in the design of trenchless rehabilitation installations without the need for arbitrary knockdown factors.

Acknowledgments

This material is based upon work supported by the National Science Foundation under Grant No. 9978634 and Pipe Rehabilitation Council contract OSP#99-261. The financial support is appreciated. The technical advice provided by the Pipe Rehabilitation Council is gratefully acknowledged.

References

[1] Boot, J. C. and Welch, A. J., "Creep Buckling of Thin-walled Polymeric Pipe Linings Subject to External Groundwater Pressure," *Thin-Walled Structures*, Vol. 24, No. 3, 1996, pp. 191–210.

[2] Gabriel, L. H., "Keynote Address: Pipe Deflection—A Redeemable Asset," *Conference on Flexible Pipes*, Columbus, OH, 1990.

[3] Schrock, B. J. and Gumbel, J., "Pipeline Renewal 1997," Paper presented at *North American No-Dig '97*, Seattle, WA, April 1997.

[4] Creus, G. J., *Viscoelasticity-Basic Theory and Applications to Concrete Structures*, Springer-Verlag, New York, 1986.

[5] Straughan, W. T., Guice, L. K., and Mal-Duraipandian, C., "Long-Term Structural Behavior of Pipeline Rehabilitation Systems," *Journal of Infrastructure Systems*, Vol. 1, No. 4, 1995, pp. 214–220.

[6] Timoshenko, S. P. and Gere, J. M., *Theory of Elastic Stability*, 2nd Edition, McGraw-Hill, New York, NY, 1961.

[7] Glock, D., "Post-critical Behavior of a Rigidly Encased Circular Pipe Subject to External Water Pressure and Temperature Rise," *Der Stahlbau*, Vol. 46, No. 7, 1977, pp. 212–217.

[8] Chunduru, S. M., Barber, E., and Bakeer, R. M., "Buckling Behavior of Polyethylene Liner Systems," *Journal of Materials in Civil Engineering*, Vol. 8, No. 4, 1996, pp. 201–206.

[9] Godoy, L. A., *Thin Walled Structures with Structural Imperfections: Analysis and Behavior*, Pergamon Press, Oxford, U.K., 1998, 404 pp.

[10] Godoy, L. A., *Theory of Elastic Stability: Analysis and Sensitivity*, Taylor and Francis, Philadelphia, PA, 2000, 434 pp.

[11] Bakeer, R. M., Barber, M. E., Taylor, J. E., and Pechon, S. E., "Long-Term Buckling Performance of HDPE Liners," *Journal of Materials in Civil Engineering*, Vol. 13, No. 3, 2001, pp. 176–184.

[12] Bakeer, R. M., Barber, M. E., Pechon, S. E., Taylor, J. E., and Chunduru, S., "Buckling of HDPE Liners Under External Uniform Pressure," *Journal of Materials in Civil Engineering*, Vol. 11, No. 4, 1999, pp. 353–361.

[13] Mahalingam, R., *A Viscoelastic Model to Determine the Long-Term Buckling Pressure of CIPP Liners*, M.S. Thesis, Louisiana Tech. University, Ruston, LA, 1996.

[14] Aalders, A. C., Bakeer, R. M., and Barber, M. E., "Deformation Measurement of Liners During Buckling Tests," *Proceedings of the Conference on Trenchless Pipeline Projects*, 1997, pp. 327–334.

[15] Moore, I. D. and Hu, F., "Linear Viscoelastic Modeling of Profiled High Density Polyethylene Pipe," *Canadian Journal of Civil Engineering*, Vol. 23, No. 2, 1996, pp. 395–406.

[16] Farshad, M. and Flueler, P., "Buckling Resistance of Polymer Pipes Under Hydrostatic Pressure," *Plastics, Rubber and Composite Processing and Applications*, Vol. 25, No. 8, 1996, pp. 373–379.

[17] Barbero, E. J. and Ford, K. J., "Equivalent Time Temperature Model for Physical Ageing and Temperature Effects on Polymer Creep and Relaxation," *ASME Journal Eng. Mat. and Technology*, Vol. 126, pp. 413–410.

[18] Barbero, E. J. and Ford, K. J., "Determination of Ageing Shift Factor Rates for Field-Processed Polymers," *SAMPE Journal of Advanced Materials*, 2005.

[19] Barbero, E. J. and Julius, M. J., "Time-Temperature-Age Behavior of Commercial Polymer Blends and Felt Filled Polymers," *Journal of Mechanics of Advanced Materials and Structures*, Vol. 11, No. 3, pp. 287–300.

[20] Struick, L. C. E., *Physical Aging in Amorphous Polymers and Other Materials*, Elsevier, Delft, The Netherlands, 1978.

[21] Rangarajan, S., *Long Term Creep of Encased Polymer Liners*, Thesis, West Virginia University, 2001.